Rupture, Fracture and size issues

E. Barthel

Surface du Verre et Interfaces

2010 / Mecano

Lignes directrices

The ultimate downscaling...Theoretical strength(s)

- Theoretical tensile strength

Energy picture – Brittle and semi-brittle fracture

- General considerations
- Downscaling

Stress concentration and Process zone – Plastic deformation at the crack tip

- Stress distribution around the crack tip
- Process zone and downscaling

Lignes directrices

Rigid surfaces – the Orowan estimate

Assume loading *on* surfaces

$$
\begin{aligned}
\sigma(z) &= E\frac{z}{\Delta} \\
V_{el}(z)/A &= E\frac{z^2}{2\Delta} = \frac{\sigma^2\Delta}{2E}
\end{aligned}
$$

Rupture occurs when $\sigma(z_{rupt}) \equiv \sigma_{theo}$ is such that $V_{el} \simeq w$

$$\sigma_{theo} \simeq \sqrt{\frac{2Ew}{\Delta}} \tag{1}$$

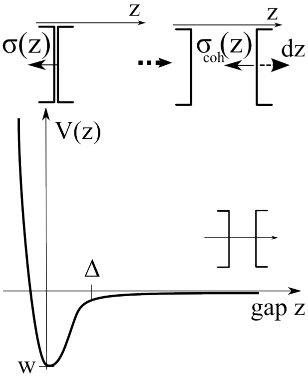

Figure: Interaction energy as a function of surface separation

After Lawn 1975 [1]

Theoretical strength

For order of magnitudes:

$$
\begin{aligned}
w &\simeq 1\ \mathrm{Jm}^{-2} \\
\Delta &\simeq 0.2\ \mathrm{nm} \\
E &\simeq 100\ \mathrm{GPa} \\
\sigma_{theo} &\simeq 30\ \mathrm{GPa}
\end{aligned}
$$

or 100 tons $= 10^6$ N on 1×1 cm^2 !!!

Does it conform to our experience ?

1. gravity against surface forces
2. balance gives surface win if

$$R^2 < w/\rho g$$

3. Cut-off radius around 1 mm !!!

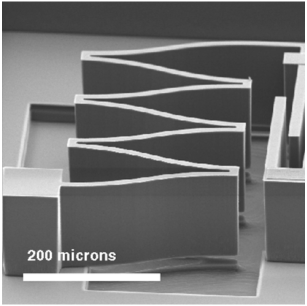

Figure: A typical MEMS

There is something more to it...roughness

What if remote loading ?

MD simulations of silica rupture

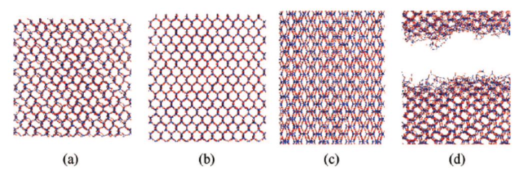

Figure: Structure

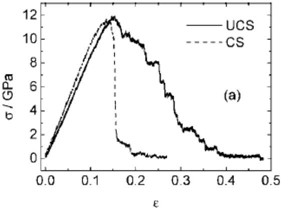

Figure: Stress

From Pedone 2008 [2]

Assuming remote loading...

- the stress is homogeneous through the macroscopic body
- predicts simultaneous rupture of the full volume when

$$\sigma_{theo} \simeq \sqrt{\frac{2Ew}{\Delta}}$$

Problem

1. Rupture does not (usually) happen that way $\rightarrow$ localized
2. We need to examine the loading and the stress distribution

Assuming remote loading...

- the stress is homogeneous through the macroscopic body
- predicts simultaneous rupture of the full volume when

$$\sigma_{theo} \simeq \sqrt{\frac{2Ew}{\Delta}}$$

Problem

1. Rupture does not (usually) happen that way $\rightarrow$ localized
2. We need to examine the loading and the stress distribution

Similar estimates for theoretical shear strength

- voir les cours de Benoit Devincre et Marc Legros

Can we measure the theoretical tensile strength directly ?

1. Surface forces measurements with fine tips allow for direct measurement of local inter-surface interactions
2. note long range contribution

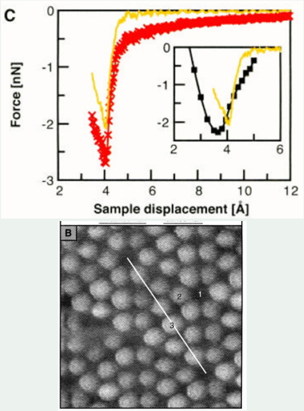

Figure: Tip/surface interaction.

After Lanz 2001 [3]

More sophisticated...

With long range cohesive forces

$$\begin{aligned} \sigma(z) &= Az \text{ for } z \ll \Delta \\ \sigma(z) &= Cz^{-3} \text{ for } z \gg \Delta \end{aligned}$$

Rupture occurs when $\sigma(z_{rupt}) \equiv \sigma_{theo}$ is of the order

$$\sigma_{crit} \simeq (A^{1/3}C)^{1/4}$$

Ref. Kohn 1979 [4]

Lignes directrices

Fracture: the energy release rate

Bottom line

- A very unstable geometry : fracture
- How much energy is available ? = stability criterion for the fracture

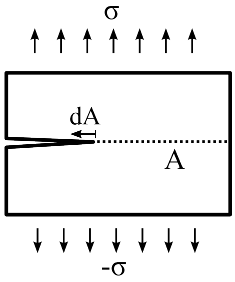

Figure: A crack with some remote loading.

Energy Release Rate – Peeling

- Energy balance:

$$-F \; da = -w \; b \; da$$

- Energy release rate:

$$\mathcal{G} = F/b = w$$

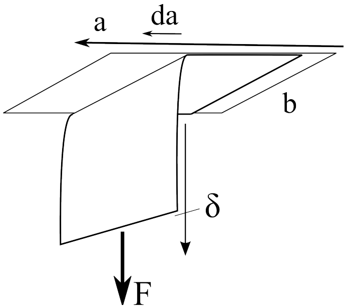

Figure: Peeling at 90°.

- No elastic deformation energy
- simplest example ever

Energy release rate – Calculation

A bit of technique

Method

- equilibrium solution including co/ad-hesive energy
- from potential energy minimization

Potential Energy Minimization
A 1-element model

- from potential energy minimization
- a simple example

$$
\begin{aligned}
\mathcal{E} &= \frac{k}{2}(u-u_0)^2 - uF \\
d\mathcal{E} &= k(u-u_0)du - duF
\end{aligned}
$$

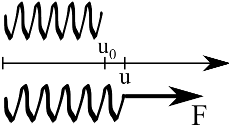

Figure: A simple spring system under tension.

Equilibrium

The equilibrium value of u obeys $d\mathcal{E} = 0$ for all du or

$$F = k(u-u_0)$$

Potential Energy Minimization
A 1-element model

- from potential energy minimization
- a simple example

$$\begin{aligned}\mathcal{E} &= \frac{k}{2}(u-u_0)^2 - uF \\ d\mathcal{E} &= k(u-u_0)du - duF\end{aligned}$$

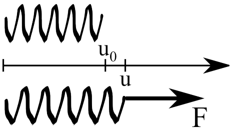

Figure: A simple spring system under tension.

Equilibrium

The equilibrium value of u obeys $d\mathcal{E} = 0$ for all du or

$$F = k(u-u_0)$$

SAINT-GOBAIN

Energy release rate – Energy balance

- from potential energy minimization
- fracture: general case

$$
\begin{aligned}
\mathcal{E} &= \mathcal{E}_{el} - \left\{ \int_{surf} u\sigma dS \right\} \\
d\mathcal{E} &= 0
\end{aligned}
$$

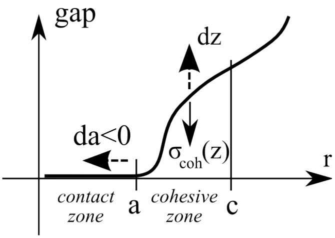

Figure: Schematics of the cohesive zone

Contribution from the cohesive stresses

$$
d\left\{ \int_{surf} u\sigma dS \right\} = \int_0^\infty \sigma_{coh}(z) dz dA = w dA
$$

Energy release rate – Energy balance

- from potential energy minimization
- fracture: general case

$$\begin{aligned} \mathcal{E} &= \mathcal{E}_{el} - \left\{ \int_{surf} u\sigma dS \right\} \\ d\mathcal{E} &= 0 \end{aligned}$$

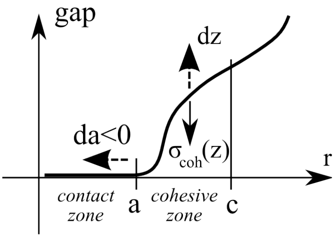

Figure: Schematics of the cohesive zone

Contribution from the cohesive stresses

$$d\left\{ \int_{surf} u\sigma dS \right\} = \int_0^\infty \sigma_{coh}(z) dz dA = w dA$$

Bottom line

- Energy release rate – working definition

$$\mathcal{G} \equiv \left.\frac{d\mathcal{E}_{el}}{dA}\right|_{\delta}$$

or

$$\mathcal{G} \equiv \left.\frac{d(\mathcal{E}_{el} - F\delta)}{dA}\right|_{F}$$

- At equilibrium

$$\mathcal{G} = w$$

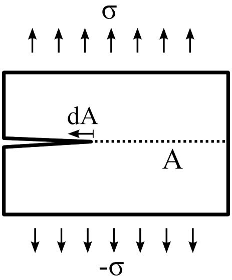

Figure: A crack with some remote loading.

A non-trivial example – the Double Cantilever Beam

$$F = \alpha\delta \quad \text{with} \quad \alpha = \frac{Eb}{4}\left(\frac{h}{L}\right)^3$$

$$\mathcal{E}_{el}(\delta, A) = \frac{1}{2}\alpha\delta^2$$

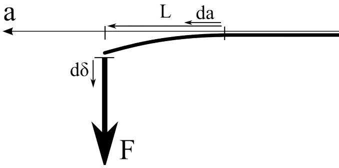

Figure: DCB.

Energy release rate

$$\mathcal{G} = \frac{3Eh^3}{8}\frac{\delta^2}{L^4} \text{ at fixed grip}$$

and

$$\mathcal{G} = \frac{6}{Eh^3}L^2\left(\frac{F}{b}\right)^2 \text{ at fixed load}$$

AIN

A non-trivial example – the Double Cantilever Beam

$$F = \alpha\delta \quad \text{with} \quad \alpha = \frac{Eb}{4}\left(\frac{h}{L}\right)^3$$

$$\mathcal{E}_{el}(\delta, A) = \frac{1}{2}\alpha\delta^2$$

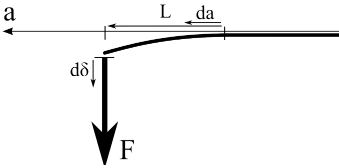

Figure: DCB.

Energy release rate

$$\mathcal{G} = \frac{3Eh^3}{8}\frac{\delta^2}{L^4} \text{ at fixed grip}$$

and

$$\mathcal{G} = \frac{6}{Eh^3}L^2\left(\frac{F}{b}\right)^2 \text{ at fixed load}$$

- fixed grip is isochoric
- fixed load is isobaric

Energy landscape – Stability

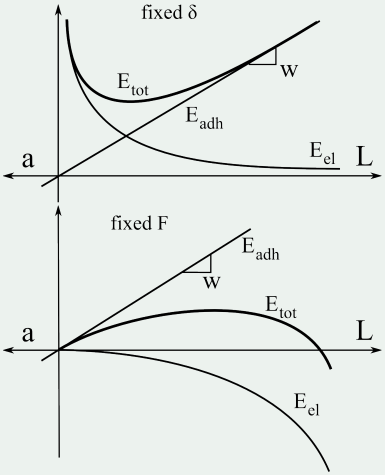

Figure: DCB at fixed grip (top) and fixed load (bottom).

cf Maugis 2000 [5]

double cantilever beam – Application

thin film adhesion

- glass substrate and backing
- multilayers deposited on the substrate

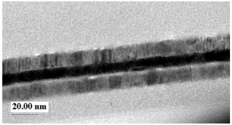

After Barthel 2005 [6]

Interface toughness measurements

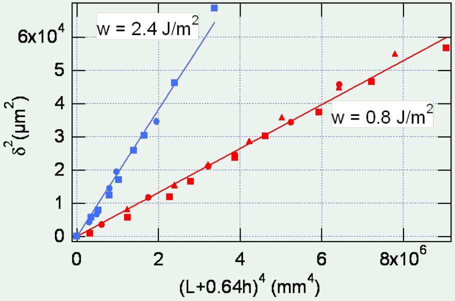

Figure: Application of DCB test for thin film adhesion measurements.

Crack branching – the Cook Gordon mechanism

$$\sigma = \sqrt{\frac{E^\star w_{coh}}{\pi h}} \quad \text{and} \quad \sigma = \sqrt{\frac{4 E w_{int}}{h}} \qquad (2)$$

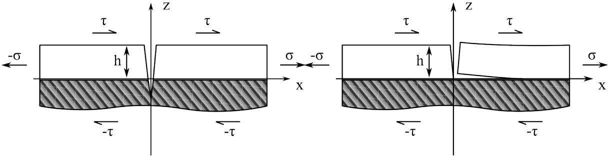

Figure: Branching criterion for coating fracture.

Interface delamination

$$w_{coh} > 4\pi w_{int}$$

SAINT-GOBAIN

Crack branching – the Cook Gordon mechanism

$$\sigma = \sqrt{\frac{E^\star w_{coh}}{\pi h}} \quad \text{and} \quad \sigma = \sqrt{\frac{4 E w_{int}}{h}} \tag{2}$$

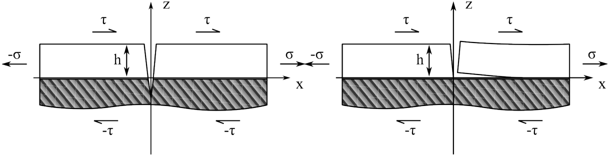

Figure: Branching criterion for coating fracture.

Interface delamination

$$w_{coh} > 4\pi w_{int}$$

Energy release rate – the general case

Full 3D fracture

Energy release rate:

$$\mathcal{G} = \psi \frac{\sigma^2 a}{E}$$

where ψ is a numerical constant of the order of 1

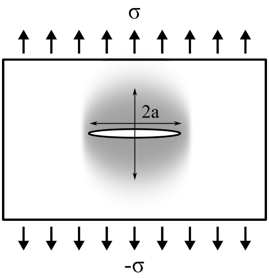

Figure: A 3D crack – half-penny.

Remote loading at rupture

$$\sigma \simeq \sqrt{\frac{Ew}{a}} \tag{3}$$

AIN

Energy release rate – the general case

Full 3D fracture

Energy release rate:

$$\mathcal{G} = \psi \frac{\sigma^2 a}{E}$$

where ψ is a numerical constant of the order of 1

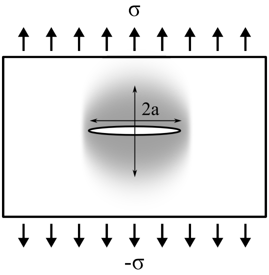

Figure: A 3D crack – half-penny.

Remote loading at rupture

$$\sigma \simeq \sqrt{\frac{Ew}{a}} \tag{3}$$

AIN

Size effects in rupture

Glass

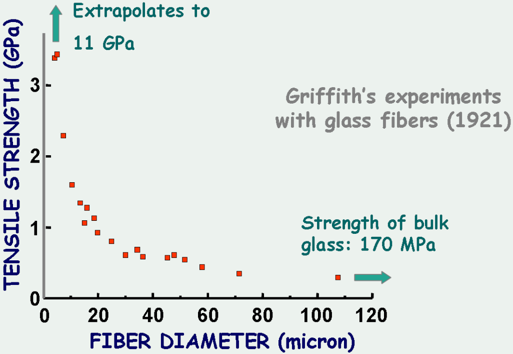

Figure: Tensile strength – Griffith's data.

After Griffith 1921 [7]

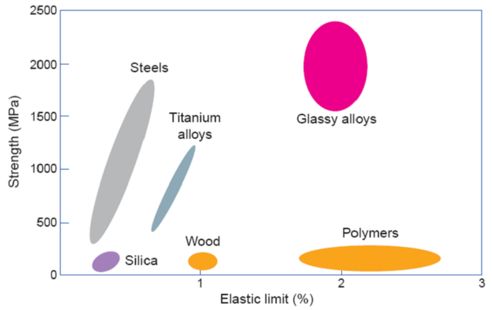

Fig. 3 Amorphous metallic alloys combine higher strength than crystalline metal alloys with the elasticity of polymers.

Figure: Strength distribution as a function of "elastic limit" for various materials.

After Telford, Materials Today, March 2004.

Ultimate tensile strain

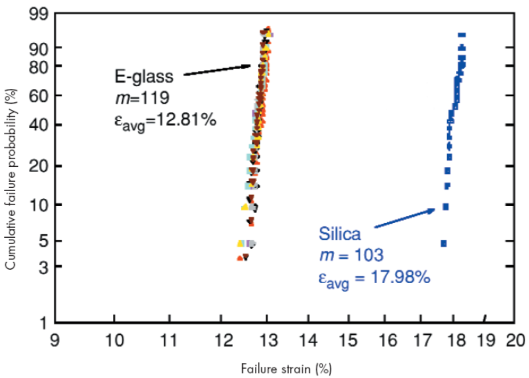

Figure: Rupture strain distribution for glass and silica fibers.

After Brow 2005 [8]

Glass fibers

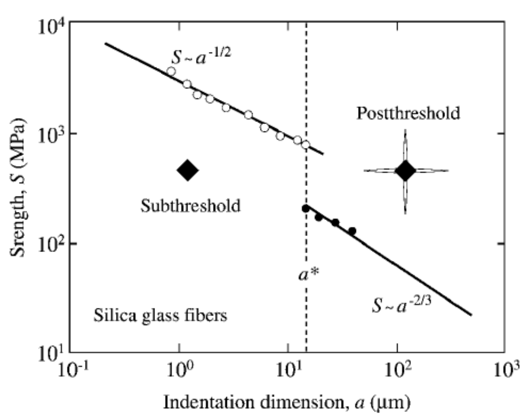

Figure: Failure strength as a function of defect size and nature.

After Lin 1996 [9]

Semi-brittle materials

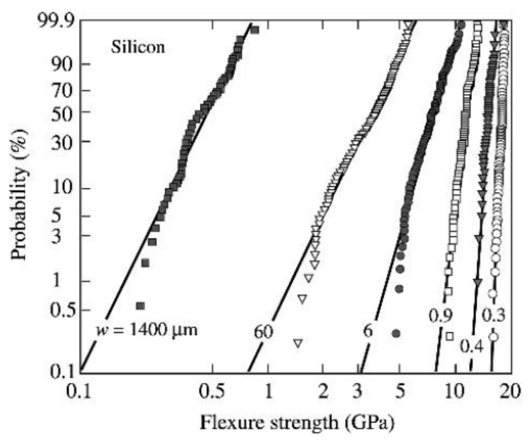

Figure: Failure distribution as a function of size of Si beam.

After Namazu 2000 [10]

Lignes directrices

Pulling out a punch on a film

$$F = \pi a^2 E \left(\frac{d}{h}\right)$$

$$\mathcal{E} = \pi a^2 h \times \frac{1}{2} E \left(\frac{d}{h}\right)^2$$

$$\mathcal{G} = \frac{\partial \mathcal{E}}{\partial \pi a^2} = w$$

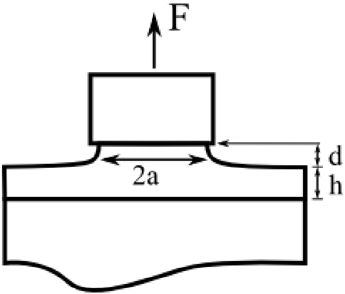

Rupture

- displacement:

$$w = \frac{Ed^2}{2h}$$

- mean stress

$$\sigma = \sqrt{\frac{2Ew}{h}} \quad (4)$$

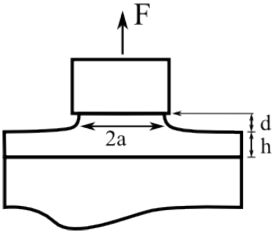

Figure: Punch on a thin film

The glue salesman paradox (Kendall 2001 [11])

The less glue the more it sticks (*ie* the larger the pull-out force)

1

[1] The *energy* at rupture $\int Fdd = w$ but is difficult to measure (instrument stiffness)

Experimental results

1. Pull out test on cylindrical dies
2. Variable glue joint thickness

The Merril Meissner data

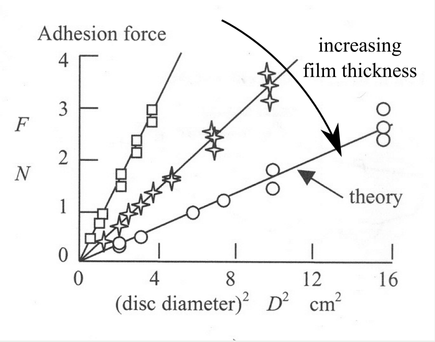

Figure: Pull out force

After Kendall 2001 [11]

Substrate constraint on film cracking

Energy release rate

a) $\mathcal{G} = \psi_0 \dfrac{\sigma^2 a}{E}$

b) $\mathcal{G} = \psi_1 \dfrac{\sigma^2 h}{E}$

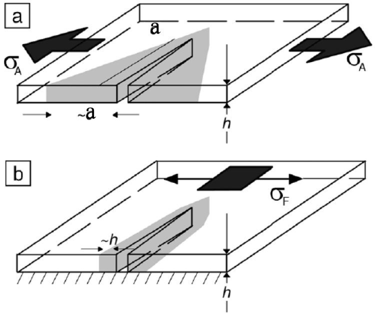

Figure: Substrate constraint on thin films.

After Cook 2002 [12]

Impact of substrate constraint – compliant interlayer

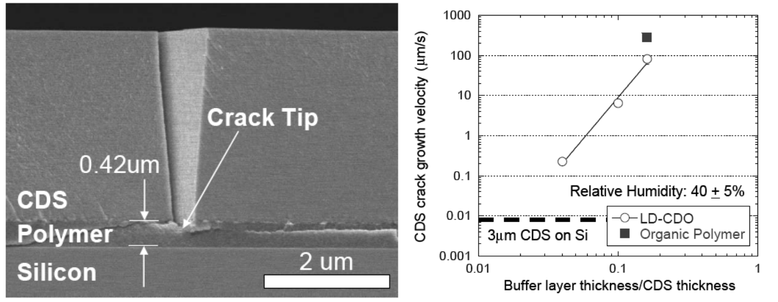

Figure: Cross section (left) and crack velocity (right)

After Tsui 2005 [13]

Lignes directrices

The ultimate downscaling...Theoretical strength(s)

- Theoretical tensile strength

Energy picture – Brittle and semi-brittle fracture

- General considerations
- Downscaling

Stress concentration and Process zone – Plastic deformation at the crack tip

- Stress distribution around the crack tip
- Process zone and downscaling

Antiplane elasticity

Same quality, lower price...

Elastic fields and equilibrium

- deformation and stress

$$\bar{\epsilon} = \nabla u(x, y)$$

$$\bar{\sigma} = \mu \bar{\epsilon}$$

- equilibrium

$$\mathrm{div}(\bar{\sigma}) = 2\mu \triangle(u)$$

$$\Delta u = 0$$

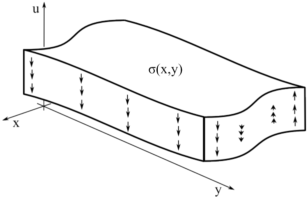

Figure: Deformation for antiplane elasticity

Boundary conditions

Boundary conditions

- stress

$$\sigma_y = 0 \quad \text{for} \quad \theta = \pm\pi$$

- u is discontinuous on the fracture faces

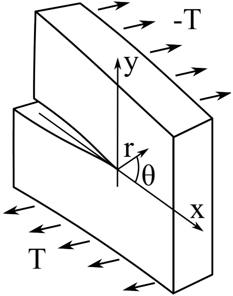

Figure: Fracture geometry in mode III

$$u = \mathcal{I}m(\Omega) \quad \text{with} \quad \Omega = Az^{1/2}$$

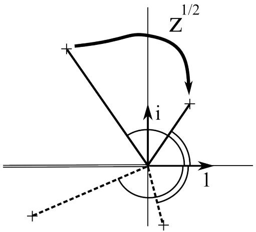

Figure: The stress distribution around the crack tip.

$$\sigma_x = -A\mu/2r^{-\frac{1}{2}} \sin(\theta/2)$$
$$\sigma_y = A\mu/2r^{-\frac{1}{2}} \cos(\theta/2)$$

Crack tip stress field

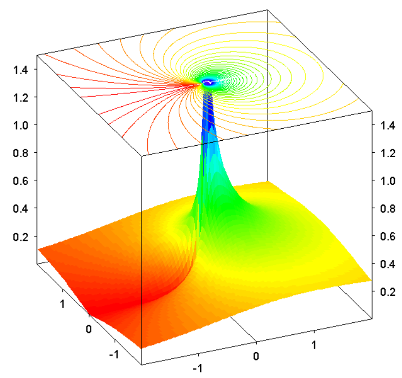

Figure: The stress distribution around the crack tip.

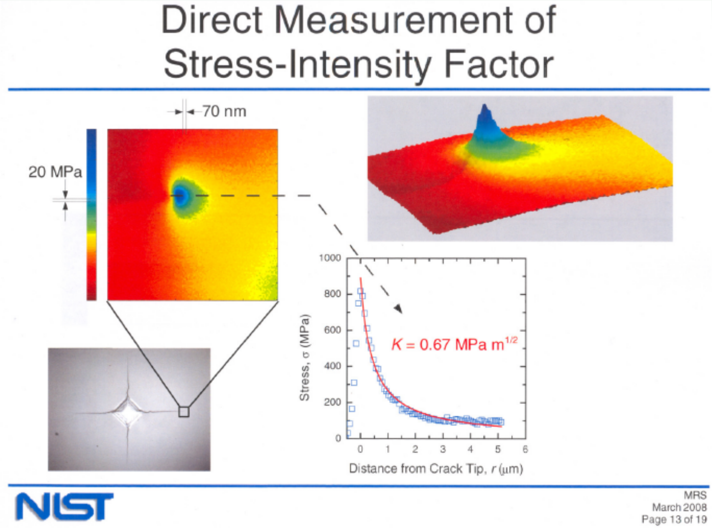

Figure: Measured crack tip stress field. After Cook 2008

Connexion to the macroscopic lengthscale

With $K = A\mu$

$$\mathcal{G} = \frac{\pi}{2}\frac{K^2}{2\mu}$$

A slit crack

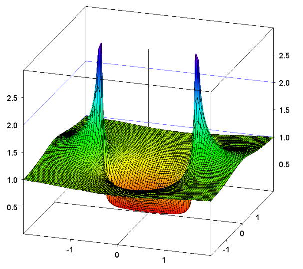

Figure: Stress field distribution σ_y

The lower lengthscale problem

$$\sigma_{coh} \simeq \sqrt{\frac{Ew}{\epsilon}} \qquad (5)$$

Cohesive zone

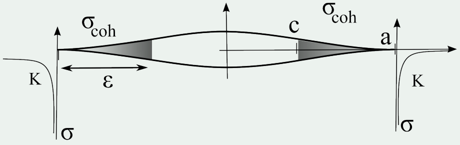

Figure: Cohesive stress and singularity regularization / Barenblat-Dugdale model

The lower lengthscale problem

Animal pad division

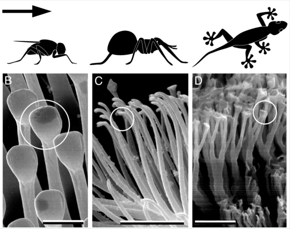

Figure: Various pads as a function of species.

Size Effect

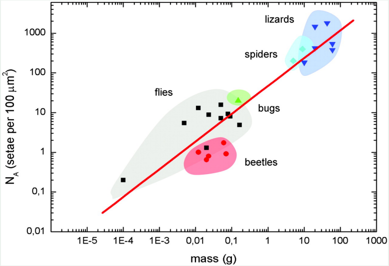

Figure: Pad division as a function of weight.

After Arzt 2003 [14]

The lower lengthscale problem

Animal pad division

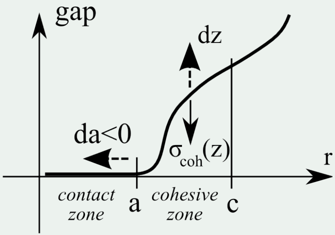

Figure: Cohesive zone.

Average stress

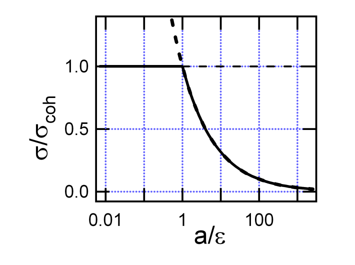

Figure: Cut-off with size reduction.

After Arzt 2003 [14]

Lignes directrices

The ultimate downscaling...Theoretical strength(s)

- Theoretical tensile strength

Energy picture – Brittle and semi-brittle fracture

- General considerations
- Downscaling

Stress concentration and Process zone – Plastic deformation at the crack tip

- Stress distribution around the crack tip
- Process zone and downscaling

Rupture and macroscopic plasticity

- plastic dissipation contributes to the (steady state) effective toughness Γ_{ss}
- extends over radius R_{ss}
- yield stress:

$$\sigma_y \simeq \sqrt{\frac{\Gamma_{ss} E}{R_{ss}}} \qquad (6)$$

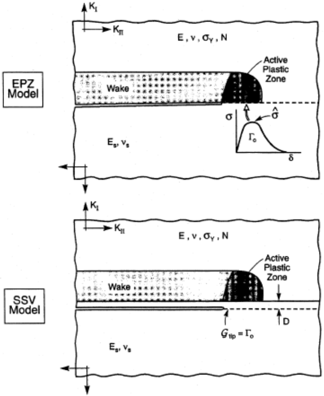

Figure: Two models for plastic dissipation

After Wei 1999 [15]

voir cours de Samuel Forest

Plastic process zone

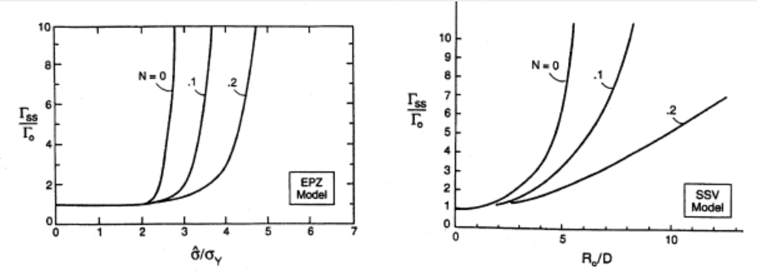

Figure: Toughness as a function of peak stress.

From Wei 1999 [15]

Toughness as a function of confinement

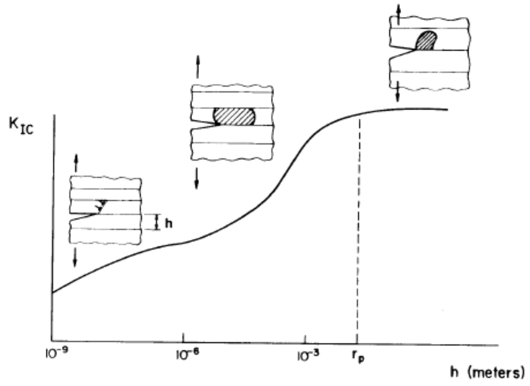

Figure: Three regimes of confinement.

From Hsia 1994 [16]

- Cu film
- Mao model based on [16]
- Present model based on:

$$\sigma_y = \sigma_{y0}\left(1 + \frac{\beta}{\sqrt{h}}\right)$$

From Volinsky 2002 [17]

Contribution of plastic dissipation

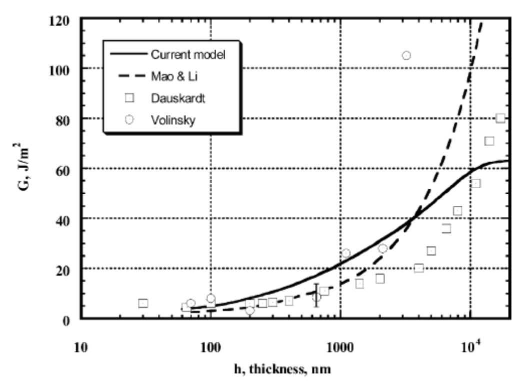

Figure: Interfacial toughness as a function of film thickness

Size and strength – from Richter 2009 [18]

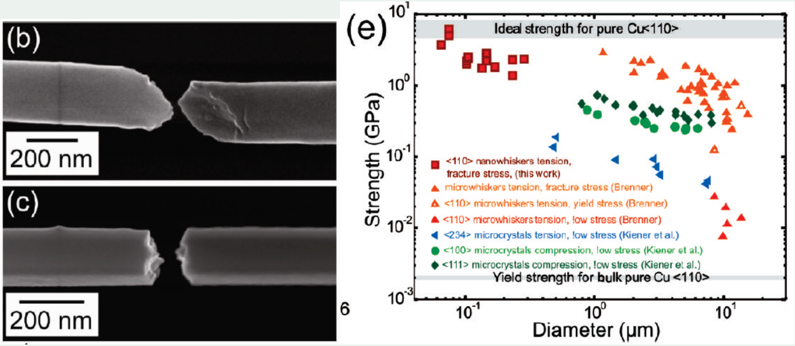

Tensile strength of Cu whiskers

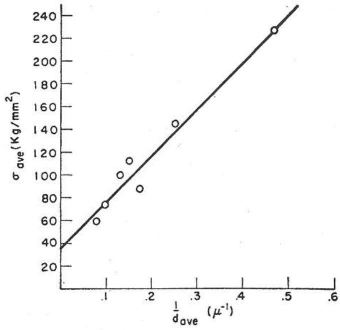

FIG. 10. The average strength of copper whiskers as a function of the reciprocal of the diameter.

From Brenner 1956 [19]

In 1858, KARMARSCH* found that the tensile strength of metal wires could be represented within a few per cent. by an expression of the type

$$\mathbf{F} = \mathrm{A} + \frac{\mathrm{B}}{d} \quad \ldots \ldots \ldots \quad (22)$$

where d is the diameter and A and B are constants.

From Griffith 1921 [7]

Conclusion

Rupture

Beyond the physical rupture mechanisms at the interface

- intrinsically spans lengthscales
- intrinsically spans stress ranges
- involves specific material response

B. Lawn and T. Wilshaw.
Fracture of Brittle Solids.
CUP, 1975.

A. Pedone, M. A. L. A. V. A. S. I. Gianluca, C.-M. M, S. E. G. R. E. Ulderico, and C. A. N.
Molecular Dynamics Studies of Stress-Strain Behavior of Silica Glass under a Tensile Load.
Chem. Mater., 20(21957):4356 – 4366, 2008.

M. A. Lantz, H. J. Hug, R. Hoffmann, P. J. A. Van Schendel, P. Kappenberger, S. Martin, A. Baratoff, and H.-J. Güntherodt.
Quantitative measurement of short-range chemical bonding forces.
Science, 291:2580–2583, 2001.

W. Kohn and A. Yaniv.
Universal model for the surface energy of solids.
Physical Review B, 20(12):4948–4952, 1979.

D. Maugis.
Contact, Adhesoin and Rupture of Elastic Solids.
Springer, Berlin Heidelberg, 2000.

E. Barthel, O Kerjan, P. Nael, and N. Nadaud.
Asymmetric silver to oxide adhesion in multilayers deposited on glass by sputtering.
Thin Solid Films, 473:272–7, 2005.

AA Griffith.
The phenomena of rupture and flow in solids.
Philosophical Transactions of the Royal Society of London. Series A, Containing Papers of a Mathematical or Physical Character, pages 163–198, 1921.

R. P. Brow, N. P. Brower, and C. P. Kurkjian.
Tpb test provides new insight to fiber strength.
American Ceramic Society Bulletin, 84:10–51, 2005.

B. Lin and MJ Matthewson.

Inert strength of subthreshold and post-threshold Vickers indentations on fused silica optical fibres.
Philosophical Magazine A, 74(5):1235–1244, 1996.

T. Namazu, Y. Isono, and T. Tanaka.
Evaluation of size effect on mechanical properties of singlecrystal silicon by nanoscale bending test using AFM.
Microelectromechanical Systems, Journal of, 9(4):450–459, 2000.

K. Kendall.
Molecular Adhesion and Its Applications.
Kluwer, New York, 2001.

R.F. Cook and Z. Suo.
Mechanisms Active during Fracture under Constraint.
MRS BULLETIN, page 45, 2002.

T.Y. Tsui, A.J. McKerrow, and J.J. Vlassak.
Constraint effects on thin film channel cracking behavior.

JOURNAL OF MATERIALS RESEARCH-PITTSBURGH THEN WARRENDALE-, 20(9):2266, 2005.

E. Arzt, S. Gorb, and R. Spolenak.
From micro to nano contacts in biological attachment devices.
Proc. Natl. Acad. Sci. USA, 100(19):8 – 10, 2003.

Y. Wei and J. W. Hutchinson.
Models of interface separation accompanied by plastic dissipation at multiple scales.
Int. J. Fract., 95:1–17, 1999.

KJ Hsia, Z. Suo, and W. Yang.
Cleavage due to dislocation confinement in layered materials.
Journal of the mechanics and physics of solids, 42:877–877, 1994.

A. A. Volinsky, N. R. Moody, and W. W. Gerberich.
Interfacial toughness measurements for thin films on substrates.
Acta Mater., 50:441 – 466, 2002.

G. Richter, K. Hillerich, D.S. Gianola, R. Monig, O. Kraft, and C.A. Volkert.
Ultrahigh Strength Single Crystalline Nanowhiskers Grown by Physical Vapor Deposition.
Nano Letters, pages 45–73, 2009.

SS Brenner.
Tensile strength of whiskers.
Journal of Applied Physics, 27:1484, 1956.